Chapter 4

Results and Discussion

4.1 Two Stages Measurement System Setup

We divide the experiment into two stages, to optimize the power budget for an MZM. The first stage is to determine the best input optical power level for an MZM. The input power is varied to finds highest converted RF extinction ratio. In the second stage, the obtained input power level is applied. The tunable gain-controlled EDFA is used to provide the different constant two-tone optical levels, to finds highest converted RF extinction ratio again.

4.1.1 The Best Input Optical Power Level

From our experiment, we consider the two-tone signals by considering the converted RF extinction ratio by an RF spectrum analyzer. The 1st harmonic should be lowest and the required 2nd harmonic should be highest simultaneously. The converted RF extinction ratio values between the 1st and the 2nd harmonic are shown in figure 4.1. The blue line is the maximum while the red line is the minimum extinction ratio. The X axis is the input optical power level from 6 to 14 dBm. The Y axis is the extinction ratio in dBm unit. The results show that the extinction ratio increases as input optical power increases until at the 13dBm. At the optical power level are higher than 13dBm, the extinction ratio trend is decreased. It should be noted that the maximum optical input power of an MZM is 23dBm as mentioned in chapter 3, the test input optical power is achieved as high as 13dBm due to the maximum output power of the light source. From this experiment results, we conclude that the best input optical power level is 13dBm as shown in figure 4.2, and will be used to find the best output optical two-tone power level in next stage.

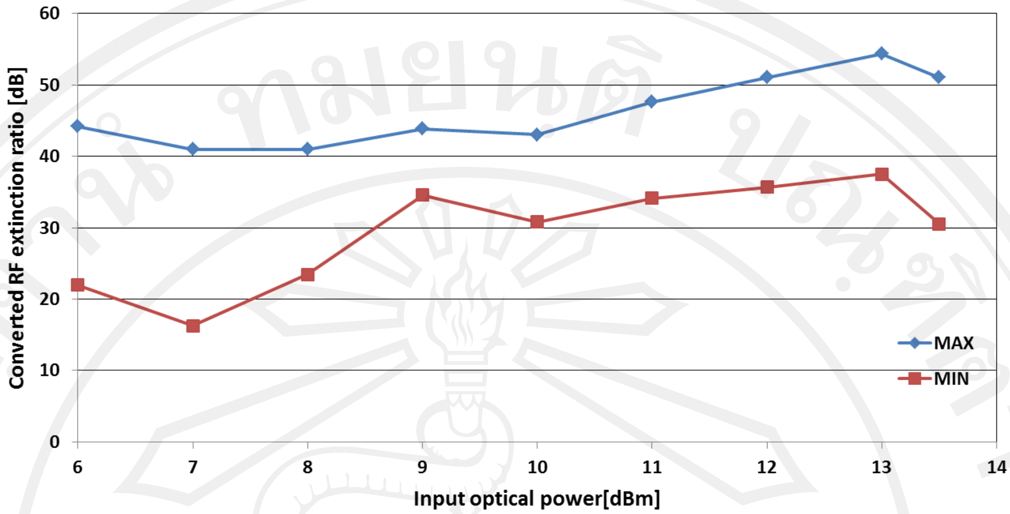

Figure 4.1 Converted RF extinction ratios as a function of the input optical power

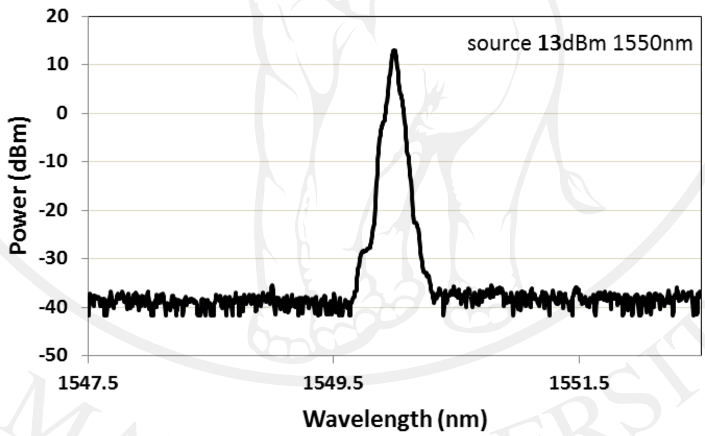

Figure 4.2 Input optical signal for the MZM

4.1.2 The Best Constant Two-tone Optical Stimulus Signal Level

The input optical power level at 13dBm from the early result is used. Due to the insertion loss of the MZM operated under null point condition, output optical power level of the MZM is about 0dBm at modulation frequency 1GHz (and will be lower than this at higher frequency) as shown in figure 4.3 which will amplify by the EDFA. By the EDFA characteristic, input optical power of 0dBm can be amplified with maximum gain about 10dB. So, the output two-tone power level should not exceed 10dBm. The converted RF extinction ratio values between the 1st and the 2nd harmonic are shown in figure 4.4.

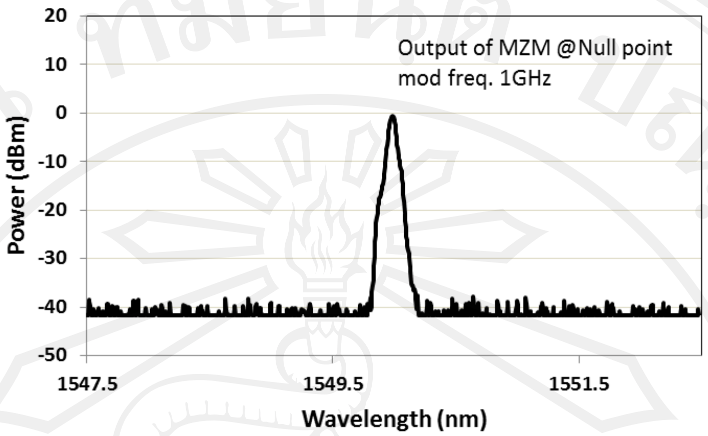

Figure 4.3 Output optical signal from the MZM with the modulation frequency at 1GHz (resolution 0.06nm)

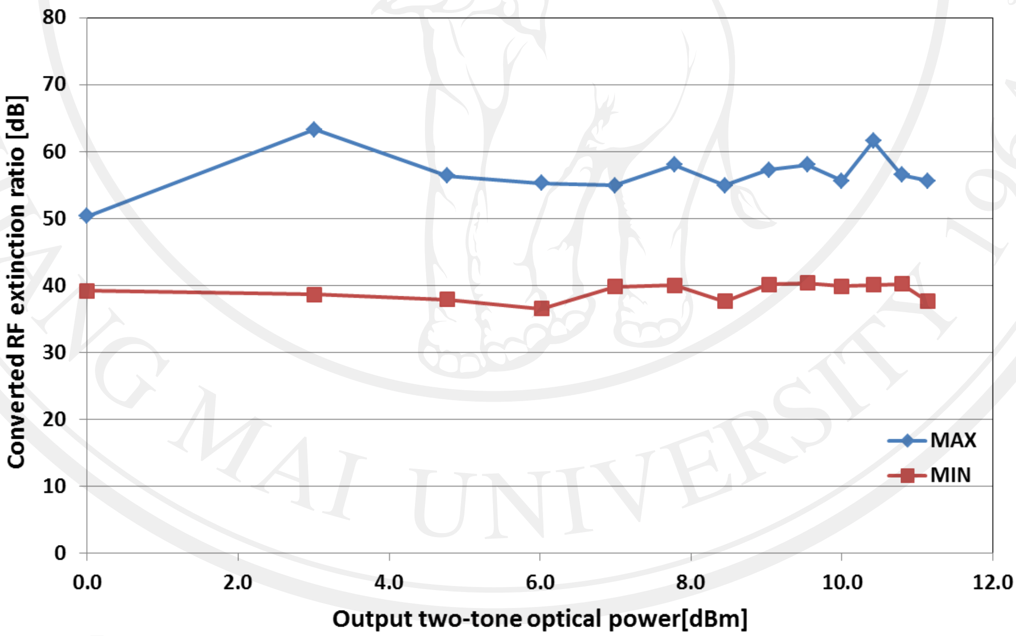

Figure 4.4 Converted RF extinction ratios as a function of the output optical two-tone power level

The blue line is the maximum while the red line is the minimum extinction ratio. The X axis is the constant output two-tone optical power level from 0 to 12 dBm. The Y axis is the extinction ratio in dBm. The results show that the maximum extinction ratio values have fluctuated around ±5dB. The optical level at below 3dBm, the extinction ratio level is lower. At power level about 3dBm, the extinction ratio is highest. At power level around 9 to 11 dBm, the minimum extinction ratio is seemed low fluctuation. From this experiment results, we therefore conclude that the best constant output optical two-tone power level higher than 3dBm is good for our PD frequency response measurement system. In this work, the constant optical two-tone power level about 7.7dBm is used as shown in figure 4.5, which is sufficiently for divided by optical couplers. Figure 4.6 is shown the converted RF extinction ratio values more than 38dB with 120 points tested frequency from 100MHZ to 12GHz. Moreover, the converted RF extinction ratio values more than 50dB can be achieved.

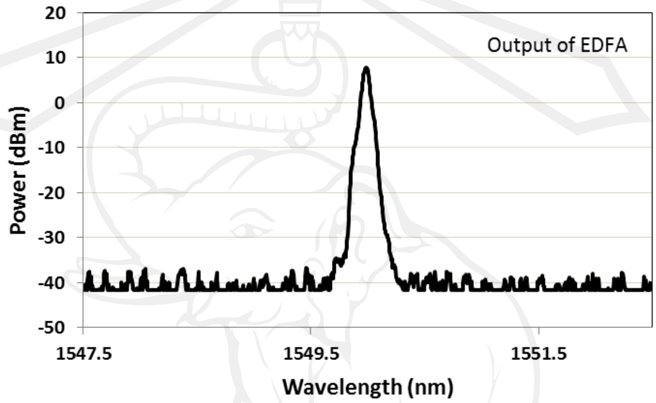

Figure 4.5 Amplified optical two-tone power by an EDFA

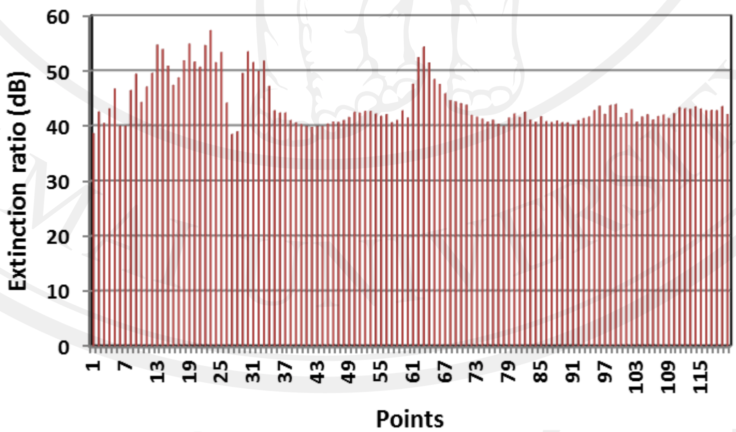

Figure 4.6 Extinction ratio of each point tested frequency (120 points)

By using the optical couplers, constant two-tone optical power level available at the PD DUT is 6dBm as shown in figure 4.7 (solid line). We observe that the noise level from the optical spectrum before (fig.4.3) and after (fig.4.5) launched into the EDFA are nearly the same about -42dBm, which is corresponding to, at the input optical power of 0dBm, the trend of the gain-saturation curves still not be the saturation region. That is shown that the effects of the ASE noise generated by an EDFA on the two-tone generation are low enough, and will not affect to the accuracy of measurement results.

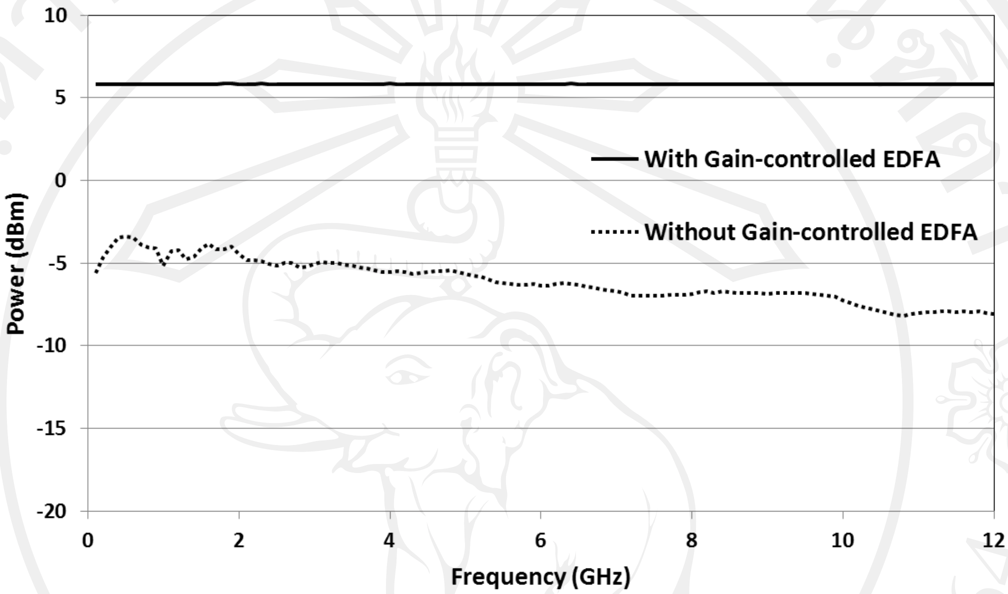

Figure 4.7 Optical two-tone powers with and without using EDFA

4.2 Compared PD Frequency Responses

Two photodiode models have tested consisting of Picometrix P-18A and Picometrix PT-15C. The frequency response results are shown below, comparing between using gain-controlled EDFA and without gain-controlled EDFA. By using gain-controlled EDFA, frequency response κ is only depending on the two powers (P_{RF} and P_{opt}) without MZM characteristic effect. The power sensor uncertainties are caused by both optical power sensor and RF power sensor. The optical power sensor discrepancies can be limited due to constant optical power and higher input optical power level. The RF power sensor error can also be decreased due to higher PD generated photocurrent level. The typical optical power sensor uncertainty (Anritsu MA9612A) is ±0.15dB [22]. The typical RF power sensor uncertainty (Agilent U2000H) is ±0.17dB [23].

4.2.1 Photodiode Model Picometrix P-18A

The frequency response result of photodiode model Picometrix P-18A (bandwidth 19GHz) is plotted in figure 4.8, with 120 points resolution from 100MHz to 12 GHz. The frequency response falls by 1dB at 12GHz. The responsivity specified in its data sheet of 0.9A/W. If electrical impedance about 50Ω of a PD and an RF power sensor are well matched, the generated photocurrent will through flow these impedance equally. Therefore, the photocurrent launch into the RF power sensor is 0.45A. The calculated response κ value is about $-6.94\,$dBe. This value is usually defined at lowest frequency of 0Hz by CW optical signal.

The result corresponds to the quoted bandwidth and responsivity of the PD. By using gain-controlled EDFA, the frequency response curve has lower fluctuation, reduced from around ±0.3dB to ±0.1dB. Although the maximum test frequency of this system is limited by the RF generator with 6 GHz maximum frequency, the technique is fully extendable to larger frequency.

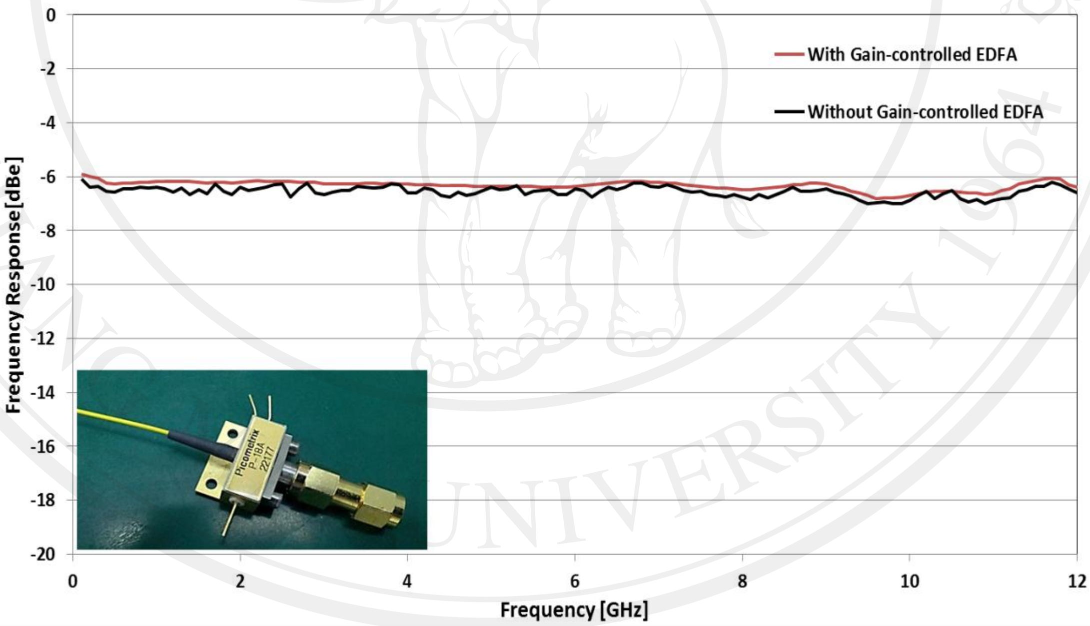

Figure 4.8 Photodiode frequency responses (Picometrix P-18A)

4.2.2 Photodiode Model Picometrix PT-15C

The frequency response result of photodiode model Picometrix PT-15C (bandwidth 15GHz) is plotted in figure 4.9, with 120 points resolution from 100MHz to 12 GHz. The frequency response falls by 3dB above 12GHz. The responsivity specified in its data sheet of 1.0A/W. If electrical impedance about 50Ω of a PD and an RF power sensor are well matched, the generated photocurrent will also through flow these impedance equally. Therefore, the photocurrent launch into the RF power sensor is 0.5A. The calculated response κ value is about $-6.02\,\text{dBe}$. From the responses result, the responsivity at the lowest frequency is about -5dBe. This may be caused by impedance mismatch or the response of this particular photodiode may be different from specification. Further measurement by LCA can be useful to determine the cause.

However, the result corresponds to the quoted bandwidth of the PD. By using gain-controlled EDFA, the frequency response curve has lower fluctuation, reduced from around ±0.3dB to ±0.1dB.

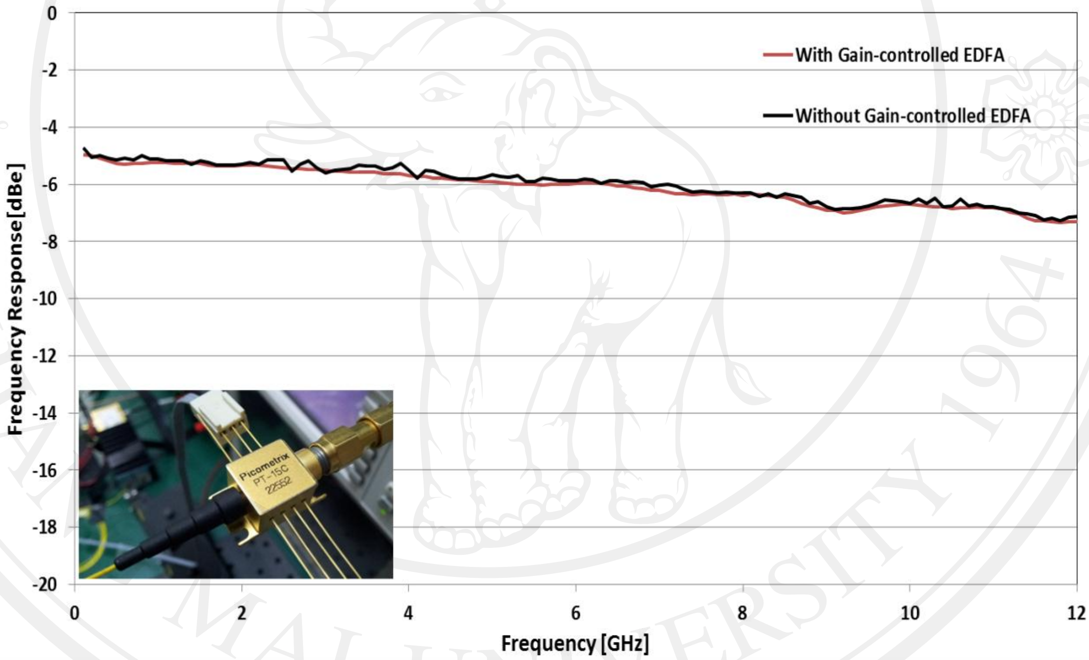

Figure 4.9 Photodiode frequency responses (Picometrix PT-15C)

4.3 Null Point Biasing Control Using LabVIEW

From the automatically controlled system, to determine the most accurate null bias point for the MZM is important to achieve the highest converted RF extinction ratio. In particular, the optical carrier is highest suppressed. So, in order to obtain the required two-tone signal, high accuracy power supply is required. And the MZM characteristic must be known for the automatic control.

4.3.1 MZM Characteristic

The MZM characteristic is obtained. By input the bias voltage from 0-12V and measure the output optical power using optical power sensor. The graph is following a sine curve as shown in figure 4.10. From this graph, we observe that the lowest transmission bias point is about 4.2V. However, the graph is shifted over time where the null point is not the same position as shown in figure 4.11. That is the reason of using the automatic computer control. Therefore, as the test frequency is swept, the new bias voltage is applied.

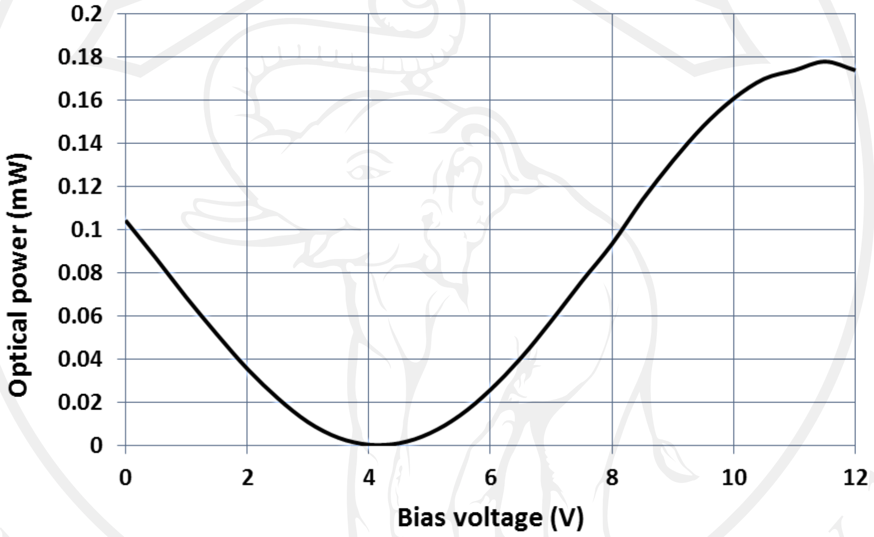

Figure 4.10 MZM characteristic as a function of bias voltages

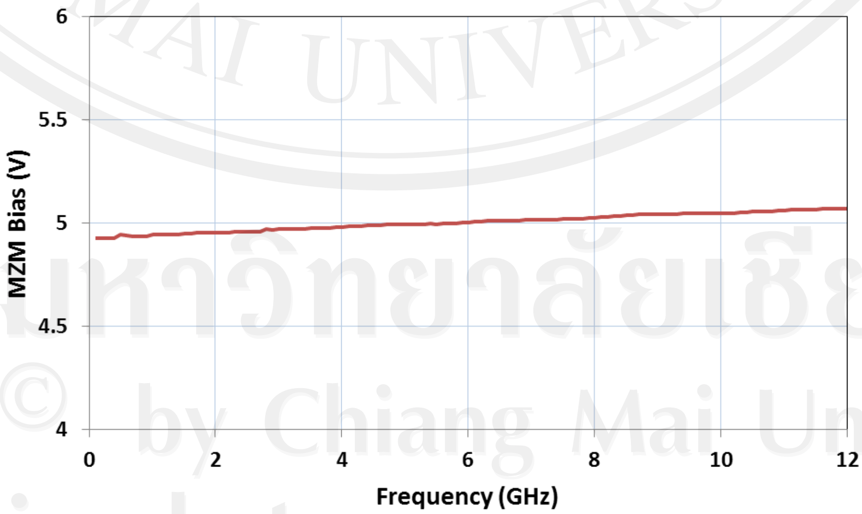

Figure 4.11 MZM bias voltages as the test frequency is swept

4.3.2 MZM Harmonics as a Function of the Bias Voltage

To obtain the null bias voltage, we has considering from the converted RF frequency component by RF spectrum analyzer instead of the optical spectrum analyzer as the original proposed [1]. The optical spectrum analyzer with resolution bandwidth of 0.01nm is required for measuring the two-tone frequency below 10GHz. As for the figure 4.10 that using the optical power sensor, it may be studied further to find null point without the RF spectrum analyzer. The main RF frequency components from the RF spectrum analyzer are consisting of 1st, 2nd and 3rd harmonic. Figure 4.12 is shown the frequency components as a function of bias voltage from 0 to 12V where the modulation frequency is kept constant at 1GHz. The blue line is the 1st harmonic. The red line is the 2nd harmonic. The green line is the 3rd harmonic. The violet line is the average RF power by RF power sensor. We observe that the 1st harmonic is lowest while the required 2nd is highest and the 3rd is lowest. As for the lowest value of the 1st and the 3rd harmonic, the beat frequency with difference frequency of 1GHz and 3GHz in the optical domain are lowest. The beat frequency with difference frequency of 2GHz in the optical domain is highest corresponding to the highest 2nd RF component. From the RF frequency components, we conclude that the null point can be found by considering only the lowest 1st point by RF spectrum analyzer. Moreover, we observe that the average RF power at the null point is nearly the same of the required 2nd value which denote that the 1st and the 3rd are sufficiently low.

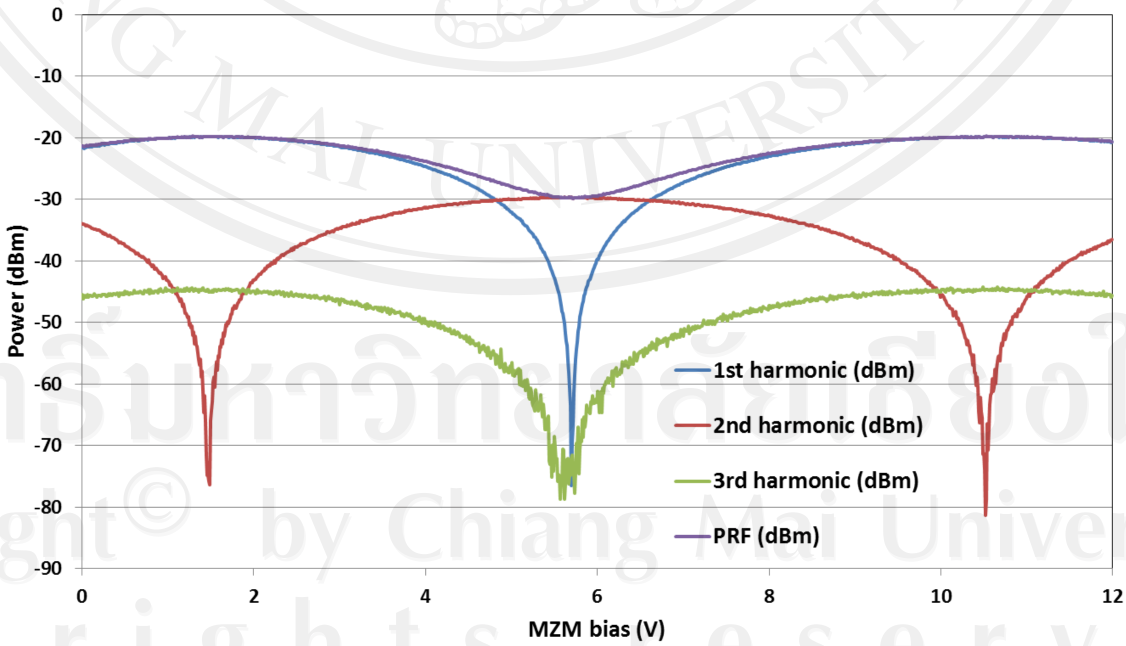

Figure 4.12 MZM harmonics as a function of bias voltages

4.3.3 Automated Null Point Biasing Control Algorithm

From the studying of the MZM characteristic, we can develop the programming algorithm by using LabVIEW for the automatic control system. In this part, we will only explain about the null point finding algorithm which is the most important as shown in figure 4.13. That is the controlling between the programmable power supply and the RF spectrum analyzer. Firstly, the initial bias voltage is get from the front panel by user, this for faster and near the null point for each MZM. The 1st harmonic value is read first. And then the bias voltage is increased by 0.1V, the 1st harmonic value is read again. The first and second readings of the 1st harmonic values are compared to find the lower value. This operation is repeated until the current value higher than the previous value. Then, the voltage resolution is changed to 0.01V for more precision. Finally, the voltage resolution is changed to 0.001V for highest precision which is the highest resolution of a power supply.

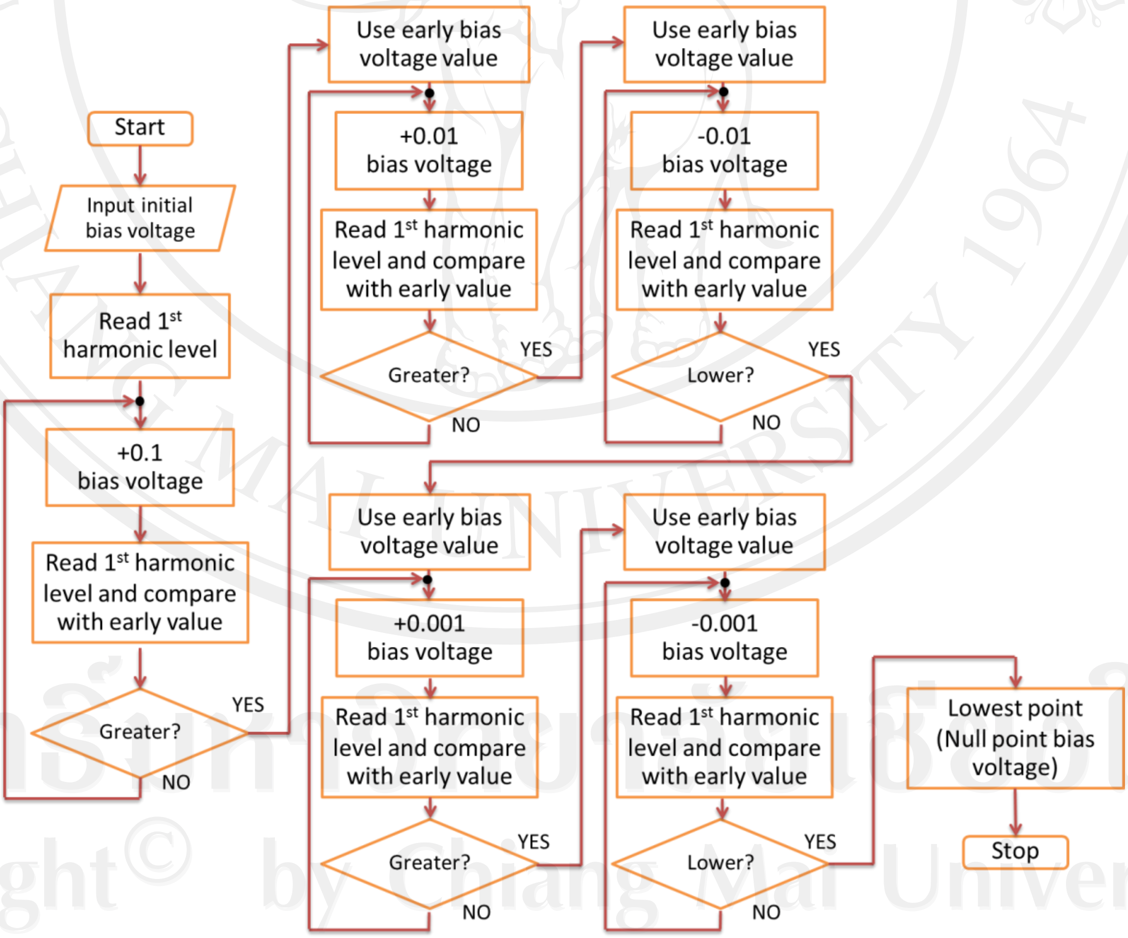

Figure 4.13 Automated null point biasing control algorithm

4. 4 ASE Noise Analysis

In previous work [4], we have demonstrated the use of EDFA to amplifying the output optical two-tone signal from an MZM and have analyzed the ASE noise as summarized below.

To estimate the ASE noise at the output of an amplifier, the amplifier is assumed to have unity coupling efficiency, uniform gain G over the optical bandwidth. The spontaneous emission power in a small optical bandwidth δv at the center frequency v in one polarization mode is given by [18]

$$P_{ASE} = n_{sp}(G-1)hv\delta v, \tag{4.1}$$

where h is the planch' constant ($6.626\times10^{-34}\, J\cdot s$) and n_{sp} is the inversion parameter defined as

$$n_{sp} = \frac{N_2}{N_2 - N_1}, \tag{4.2}$$

where N_1 and N_2 are the number of photon density in the lower state E_1 and upper state E_2 respectively. The spontaneous emission electric field E_{sp} in a filtered bandwidth B_0, as a sum of cosine terms spaced δv apart in frequency is

$$\mathrm{E_{sp}}\ (t)=\sum_{k=-B_0/2hv}^{B_0/2hv}\sqrt{2n_{sp}(G-1)hv\delta v}\cos((\omega_0+2\pi k\delta v)+\phi_k\ ). \tag{4.3}$$

If $\mathrm{N_0 = n_{sp}\,(G-1)h}\nu$ and $\mathrm{M}=\mathrm{B_0}/2\delta\nu$ are assumed. The total electric field of two-tone light plus the ASE can be expressed as

$$\mathrm{E(t)=E_{+1}(t)+E_{-1}(t)+E_{sp}(t)}. \tag{4.4}$$

$$\begin{aligned}\mathrm{E(t)}&=\sqrt{\mathrm{2GP_{+1}}}\cos(\omega_{+1}\mathrm{t})+\sqrt{\mathrm{2GP_{-1}}}\cos(\omega_{-1}\mathrm{t})\\&+\sum_{k=-M}^{M}\sqrt{2\mathrm{N_0}\delta\nu}\cos((\omega_0+2\pi k\delta\nu)+\varphi_k\ ).\end{aligned} \tag{4.5}$$

The total electric currents can be expressed as

$$\mathrm{i(t)}=\overline{\mathrm{E^2(t)}}\ \frac{\mathrm{e}}{\mathrm{h}\nu}. \tag{4.6}$$

$$i(t)=[\overline{E_{+1}^2(t)}+\overline{E_{-1}^2(t)}+\overline{E_{sp}^2(t)}+2\overline{E_{+1}(t)\,E_{sp}(t)}+2\overline{E_{-1}(t)\,E_{sp}(t)}+2\overline{E_{+1}(t)\,E_{-1}(t)}\,]\,\frac{e}{h\nu}. \tag{4.7}$$

$$\begin{aligned} i(t)= & \frac{eGP_{+1}}{h\nu}+\frac{eGP_{-1}}{h\nu}+\frac{2e}{h\nu}N_0\delta\nu[\overline{\sum_{k=-M}^{M}\cos((\omega_0+2\pi k\delta\nu)t+\varphi_k)\,]^2} \\ & +\frac{4e}{h\nu}\sqrt{GP_{+1}N_0\delta\nu}\;\overline{\sum_{k=-M}^{M}\cos(\omega_{+1}t)\cos((\omega_0+2\pi k\delta\nu)t+\varphi_k)} \\ & +\frac{4e}{h\nu}\sqrt{GP_{-1}N_0\delta\nu}\;\overline{\sum_{k=-M}^{M}\cos(\omega_{-1}t)\cos((\omega_0+2\pi k\delta\nu)t+\varphi_k)} \\ & +4G\sqrt{P_{+1}P_{-1}}\;\overline{\cos(\omega_{+1}t)\cos(\omega_{-1}t)} \end{aligned} \tag{4.8}$$

The electric currents equation (4.8) are consisting of input signal (term 1 and 2), multiplied spontaneous emission electric field with itself (term 3) referred as spontaneous- spontaneous (sp-sp) beat noise, multiplied between signal electric field and spontaneous emission electric field (term 4 and 5) referred as signal- spontaneous (signal-sp) beat noise, and the final (term 6) is multiplied between two required signal to be used for PD measurement.

Consider the signal-sp beat noise from signal P_{+1} as follow,

$$\begin{aligned} i_{+1-sp}(t) &= \frac{4e}{h\nu}\sqrt{GP_{+1}N_0\delta\nu}\;\overline{\sum_{k=-M}^{M}\cos(\omega_{+1}t)\cos((\omega_0+2\pi k\delta\nu)t+\varphi_k)} \\ &= \frac{2e}{h\nu}\sqrt{GP_{+1}N_0\delta\nu}\;\overline{\sum_{k=-M}^{M}\cos((\omega_0-\omega_{+1}+2\pi k\delta\nu)t+\varphi_k)}\;. \end{aligned} \tag{4.9}$$

The term $\omega_0+\omega_{+1}+2\pi k\delta\nu$ or nearly $2\omega_0$ is ignored because its frequency exceeds the considered frequency range. The power spectrum density can be calculated as

$$\begin{aligned} N_{+1\text{-}sp} &= \frac{1}{2}(I_{+1-sp}).2=\frac{2e^2}{(h\nu)^2}\,P_{+1}GN_0.\frac{1}{2}.2 \\ &= \frac{4e^2}{(h\nu)^2}\,P_{+1}GN_0=\frac{4e^2}{h\nu}\,P_{+1}n_{sp}(G\text{-}1)G \end{aligned} \tag{4.10}$$

Consider the signal-sp beat noise from signal P_{-1} as follow,

$$i_{-1-sp}(t) = \frac{4e}{h\nu}\sqrt{GP_{-1}N_0\delta\nu}\ \overline{\sum_{k=-M}^{M}\cos(\omega_{-1}t)\cos((\omega_0+2\pi k\delta\nu)t+\varphi_k)}$$
$$= \frac{2e}{h\nu}\sqrt{GP_{-1}N_0\delta\nu}\ \overline{\sum_{k=-M}^{M}\cos((\omega_0-\omega_{-1}+2\pi k\delta\nu)t+\varphi_k)}\ . \qquad (4.11)$$

The term $\omega_0+\omega_{+1}+2\pi k\delta\nu$ is also ignored. The power spectrum density can be calculated as

$$N_{-1\text{-sp}} = \frac{1}{2}(I_{-1-sp}).2 = \frac{4e^2}{(h\nu)^2}\ P_{-1}GN_0.\frac{1}{2}.2$$
$$= \frac{4e^2}{(h\nu)^2}\ P_{-1}GN_0 = \frac{4e^2}{h\nu}\ P_{-1}n_{sp}(G\text{-}1)G \qquad (4.12)$$

If the considered bandwidth is BW, the power spectrum of signal-sp from signal P_{+1} and P_{-1} is

$$P_{\text{signal-sp}} = \frac{4e^2}{(h\nu)^2}\ (P_{+1}+P_{-1})GN_0.BW = \frac{4e^2}{h\nu}\ (P_{+1}+P_{-1})n_{sp}(G\text{-}1)G.BW \qquad (4.13)$$

Consider the sp-sp beat noise from the square of spontaneous emission electric field as follow,

$$i_{sp-sp}(t) = \frac{2e}{h\nu}\ N_0\delta\nu\overline{[\sum_{k=-M}^{M}\cos((\omega_0+2\pi k\delta\nu)t+\varphi_k)\ ]^2}$$
$$= \frac{2e}{h\nu}\ N_0\delta\nu\overline{[\sum_{k=-M}^{M}\cos((\omega_0+2\pi k\delta\nu)t+\varphi_k)\ ][\sum_{j=-M}^{M}\cos((\omega_0+2\pi j\delta\nu)t+\varphi_j)]} \qquad (4.14)$$

$$i_{sp-sp}(t) = \frac{e}{h\nu}\ N_0\delta\nu\sum_{k=-0}^{2M}\sum_{j=-0}^{2M}\cos((k\text{-}j)2\pi k\delta\nu t+\varphi_k+\varphi_j) \qquad (4.15)$$

If the considered bandwidth is BW, the power spectrum of sp-sp beat noise is

$$P_{\text{sp-sp}} = \frac{1}{2}(\frac{e}{h\nu}\ N_0\delta\nu)^2.\frac{1}{\delta\nu}.2M.2.BW = 2n_{sp}^2\ (G\text{-}1)^2e^2B_0.BW. \qquad (4.16)$$

The total amplified optical power, but neglecting the spurious frequency components, becomes

$$\begin{aligned} p_{opt} &= \left| E_{-1}e^{j(\omega_{-1}t+\phi_{-1})} + E_{+1}e^{j(\omega_{+1}t+\phi_{+1})} + \sum_{n=-\infty}^{\infty} E_n e^{j(\omega_n t+\phi_n)} \right|^2 \\ &= |E_{-1}|^2 + |E_{+1}|^2 + 2E_{-1}E_{+1}\cos\cos(2\omega_{RF}t+\phi) \\ &+ \sum_{n=-\infty}^{\infty} |E_n|^2 + 2E_{-1}e^{j(\omega_{-1}t+\phi_{-1})} \sum_{n=-\infty}^{\infty} E_n e^{j(\omega_n t+\phi_n)} \\ &+ 2E_{+1}e^{j(\omega_{+1}t+\phi_{-1})} \sum_{n=-\infty}^{\infty} E_n e^{j(\omega_n t+\phi_n)} (n \neq -1,+1) \\ &\cong P_{opt} + P_{opt}.\cos(2\omega_{RF}t+\phi). \end{aligned} \tag{4.17}$$

The detected RF photocurrent generated by the photodiode from (2.16) change to

$$i_{RF} = \kappa.(P_{opt}\cos(2\omega_{RF}t+\phi) + P_{sig-sp} + P_{sp-sp}). \tag{4.18}$$

Since the average RF power driving a load 50Ω is

$$P_{RF} = 25 I_{RF}^2 , \tag{4.19}$$

the average extra noise in the RF power, within the bandwidth of the RF power sensor is

$$P_{error} = 25\kappa^2 (P_{sig-sp}^2 + P_{sp-sp}^2 + 2P_{opt}P_{sig-sp} + 2P_{opt}P_{sp-sp} + 2P_{sig-sp}P_{sp-sp}). \tag{4.20}$$

From the measurement data, we can estimate the RF power errors due to ASE noise detected by RF power sensor as shown below (using measurement data at 100 MHz frequency to show the calculation process).

$$P_{-1} = 7.37\ \text{dBm} \quad = \quad 5.4576\ \text{mW} \tag{4.21}$$

$$P_{+1} = 7.37\ \text{dBm} \quad = \quad 5.4576\ \text{mW} \tag{4.22}$$

Since two-tone optical power at the output of an MZM under null bias condition at modulation frequency 100MHz ($2\omega_{RF}$) is about -2.62dBm, therefore the amplifier gain G is,

$$G \approx 9.99\ \text{dB} \quad = \quad 9.977 \tag{4.23}$$

By using an optical filter, the optical bandwidth within the optical filter around the center frequency 1549.987 nm is,

$$BW = \frac{c}{\lambda^2}\partial\lambda = \frac{(3\times10^8)(1\times10^{-9})}{(1549.987\times10^{-9})^2} = 7.4923\,\text{GHz}, \tag{4.24}$$

where the center frequency v can be written as

$$v = 193.55\times10^{12}\,\text{Hz}. \tag{4.25}$$

The small frequency within the optical spectrum analyzer resolution bandwidth is

$$\delta v = \frac{c}{\lambda^2}\partial\lambda = \frac{(3\times10^8)(0.06\times10^{-9})}{(1549.987\times10^{-9})^2} = 7.4923\,\text{GHz}. \tag{4.26}$$

The estimated ASE noise power level is

$$P_{ASE} \approx -39\,\text{dBm} \qquad = \qquad 0.12589\times10^{-6}W. \tag{4.27}$$

By equation (4.1),

$$N_0 = \frac{P_{ASE}}{\delta v} = \frac{0.12589\times10^{-6}}{7.4923\times10^9} = 16.80258\times10^{-18}\ \text{W/Hz}. \tag{4.28}$$

The power spectrum of the P_{-1}- spontaneous beat noise is

$$\text{N}_{\text{-1-sp}} = \frac{4\text{e}^2}{(hv)^2}\ \text{P}_{\text{-1}}\text{GN}_0 = 5.71047\times10^{-18}\ \text{W}. \tag{4.29}$$

$$P_{-1-sp} = BW\times N_{-1-sp} = (124.872\times10^9)(5.71047\times10^{-18}) = 7.13078\times10^{-4}\ \text{mW}. \tag{4.30}$$

The power spectrum of the P_{+1}- spontaneous beat noise is

$$\text{N}_{\text{+1-sp}} = \frac{4\text{e}^2}{(hv)^2}\ \text{P}_{\text{+1}}\text{GN}_0 = 5.71047\times10^{-18}\ \text{W}. \tag{4.31}$$

$$P_{+1-sp} = BW\times N_{+1-sp} = (124.872\times10^9)(5.71047\times10^{-18}) = 7.13078\times10^{-4}\ \text{mW}. \tag{4.32}$$

The power spectrum of the spontaneous - spontaneous beat noise is

$$\text{N}_{\text{sp-sp}} = 2\left(\frac{\text{N}_0\text{e}}{hv}\right)^2 \text{B}_0 = 1.10023\times10^{-19}\ \text{mW}. \tag{4.33}$$

$$P_{sp-sp} = BW\times N_{sp-sp} = 1.37388\times10^{-8}\ \text{mW}. \tag{4.34}$$

Therefore, the power spectrum of the signal - spontaneous beat noise is

$$P_{sig-sp} = P_{-1-sp} + P_{+1-sp} = 1.42616\times10^{-3}\ \text{mW}. \qquad (4.35)$$

From the measured optical power P_{opt} at 100MHz is 4.42 dBm or 2.76694 mW, and calculated frequency response $\kappa = 0.506150198$. Therefore, the average extra noise in the RF power is

$$\begin{aligned} P_{error} &= 25\kappa^2 (P_{sig-sp}^2 + P_{sp-sp}^2 + 2P_{opt}P_{sig-sp} + 2P_{opt}P_{sp-sp} + 2P_{sig-sp}P_{sp-sp}) \\ &= 25(0.506150198)^2 (2.03392\times10^{-12} + 1.88754\times10^{-22} \\ &\quad + 7.89218\times10^{-9} + 7.60288\times10^{-14} + 3.91872\times10^{-17}) \\ &= 50.5605\times10^{-9}. \end{aligned} \qquad (4.36)$$

By using an EDFA, RF power error due to the ASE noise is below 50.561nW, which value is calculated at the lowest amplifier gain used at 100MHz modulation frequency.

From the analysis above, we can estimate additional frequency response κ errors due to ASE noise. There are two cases for consideration. In case that not using an EDFA, the RF power sensor error is ±0.196dB at RF power level of -28.56528dBm. This case gives error in κ about ±1.524136dB. In the case where EDFA is used, the RF power sensor error is ±0.195dB at RF power level of -12.89501dBm, and RF power error due to ASE noise around ±25.28nW. This second case gives error in κ about ±1.525128dB. By these two cases, ASE noise gives additional error in κ about ±0.000992dB. In table 4.1 shown the calculated RF power and frequency response errors due to ASE noise in different frequencies. As frequency increased, the RF power error due to ASE noise is decreased. At the frequency of 12GHz, the frequency response κ error is highest because of the low RF power level in case that not using an EDFA.

Table 4.1 Calculated RF power and frequency response errors due to ASE noise

Frequency (GHz)	RF power error (nW)	Additional κ error (dB)
0.1	50.561	±0.000992
4	27.696	±0.000270
8	18.107	±0.000037
12	17.958	±0.001596

4. 5 Periodic PD Frequency Response Measurements

Since optoelectronic device characteristics often depend on environment conditions, such as temperature, humidity. The absolute PD frequency response often changes with time. We have measured the PD response which is compared between using EDFA and without EDFA for two PD models as shown in figure 4.14-4.17. The change will indicate the length of time that a PD needs to be recalibrated using this proposed method. The same PDs are measured monthly both measurement schemes. The measured PD responses have consistent shapes, however the gain-controlled EDFA give better repeatability. Therefore, they need further measurement to indicate how long the time should be recalibrated. Our results indicate more than 4 months should be recalibrated.

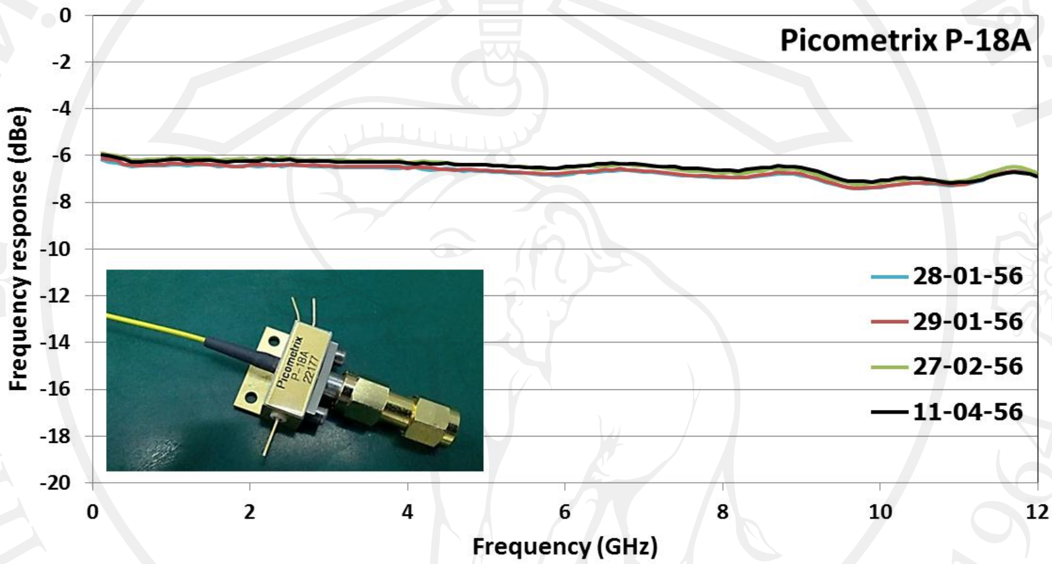

Figure 4.14 PD (Picometrix P-18A) frequency responses using gain-controlled EDFA measured at different dates

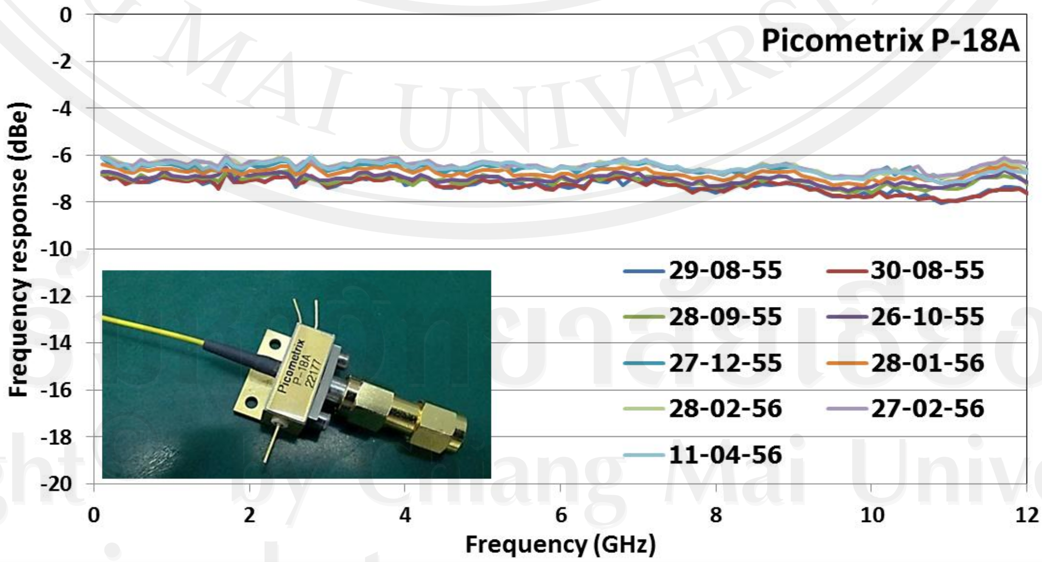

Figure 4.15 PD (Picometrix P-18A) frequency responses without using EDFA measured at different dates

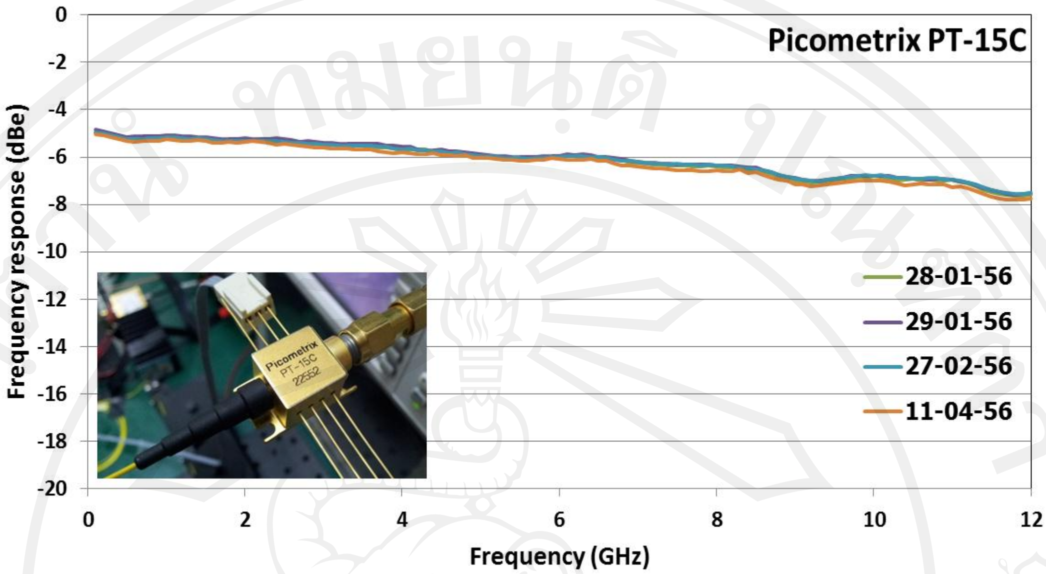

Figure 4.16 PD (Picometrix PT-15C) frequency responses using gain-controlled EDFA measured at different dates

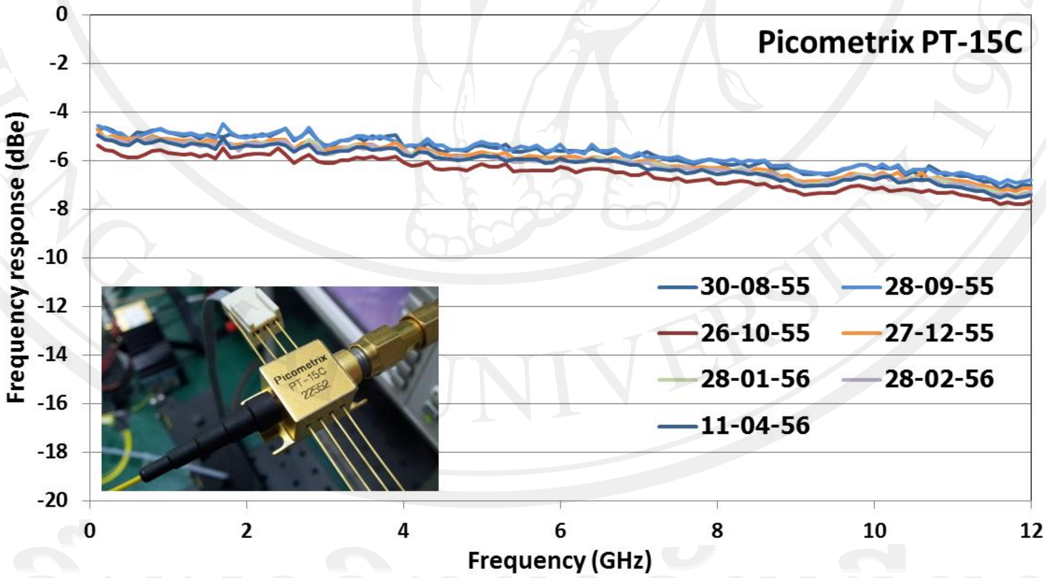

Figure 4.17 PD (Picometrix PT-15C) frequency responses without using EDFA measured at different dates